

NPEFF: NON-NEGATIVE PER-EXAMPLE FISHER FACTORIZATION

Michael Matena & Colin Raffel

Department of Computer Science
University of North Carolina at Chapel Hill
{mmatena, craffel}@cs.unc.edu

ABSTRACT

As deep learning models are deployed in more and more settings, it becomes increasingly important to be able to understand why they produce a given prediction, but interpretation of these models remains a challenge. In this paper, we introduce a novel interpretability method called NPEFF that is readily applicable to any end-to-end differentiable model. It operates on the principle that processing of a characteristic shared across different examples involves a specific subset of model parameters. We perform NPEFF by decomposing each example’s Fisher information matrix as a non-negative sum of components. These components take the form of either non-negative vectors or rank-1 positive semi-definite matrices depending on whether we are using diagonal or low-rank Fisher representations, respectively. For the latter form, we introduce a novel and highly scalable algorithm. We demonstrate that components recovered by NPEFF have interpretable tunings through experiments on language and vision models. Using unique properties of NPEFF’s parameter-space representations, we ran extensive experiments to verify that the connections between directions in parameters space and examples recovered by NPEFF actually reflect the model’s processing. We further demonstrate NPEFF’s ability to uncover the actual processing strategies used by a TRACR-compiled model. We further explore a potential application of NPEFF in uncovering and correcting flawed heuristics used by a model. We release our code to facilitate research using NPEFF.¹

1 INTRODUCTION

Neural networks trained on large datasets have achieved human-level performance on many tasks. Unfortunately, these models do not provide any direct method to understand what they have learned or how they have solved the task (Smilkov et al., 2017; Dabkowski & Gal, 2017; Sundararajan et al., 2017). This lack of interpretability can hamper progress in developing new machine learning models and can act as a hindrance to their adoption by making it hard to trust that the model’s predictions are based on sound principles (Li et al., 2022).

In this work, we propose NPEFF (Non-Negative Per-Example Fisher Factorization), an interpretability method that makes use of the model’s *parameter space* to produce representations of concepts. Our method can be used with any end-to-end differentiable model without requiring any customization to particular architectures. NPEFF extracts these concepts unsupervisedly given a set of examples. It also provides a theoretically principled way to produce guided changes in a given model’s behavior by using these concept representations to directly alter a model’s parameters.

NPEFF operates on the hypothesis that a neural network’s processing of inputs can be decomposed into a hierarchical set of abstract sub-computations. The computation performed by a model therefore makes use of a fixed set of learned sub-computations, and its processing on any particular example involves a sparse subset of them. Whether a given sub-computation is used for a given example therefore depends on the abstract concepts that underlie the example. Across examples, we assume that each sub-computation will involve a consistent subset of parameters that perform

¹https://github.com/mmatena/npeff_ref

a similar operation. Since the Fisher information matrix for each example relates perturbations in model parameters to changes in the model’s predictive distribution, the sub-computations applied to an example become imprinted in it.

NPEFF disentangles these sub-computations given a collection of per-example Fishers (PEFs) through a decomposition procedure. We provide two versions of NPEFF that operate on different representations of the PEF matrices: a diagonal approximation and an exact low-rank representation. When using diagonal PEFs, our decomposition procedure becomes equivalent to non-negative matrix factorization (NMF) (Lee & Seung, 1999). In the low rank case, we represent each example’s PEF matrix as a non-negative sum of rank-1 positive semi-definite matrices. To the best of our knowledge, this is a novel decomposition, and we introduce a scalable, multi-GPU algorithm for computing it.

The output of an NPEFF decomposition provides a direct way to quantify the importance of each component to the model’s processing of each example. Looking at the examples most influenced by a particular component provides a means to infer what concept or heuristic the component represents. Furthermore, NPEFF generates a “pseudo-Fisher” matrix for each component that can be used to estimate the impact of parameter perturbations on their associated sub-computations. By constructing perturbations that selectively impact particular components, we can verify that the components reflect how the model actually processes examples.

Overall, NPEFF provides a way to interpret a model’s processing by extracting the computational sub-steps it uses. In our experiments on text and vision models, we find that these sub-steps often corresponded to human-recognizable concepts by inspecting component top examples. Our parameter perturbation experiments demonstrate that the component pseudo-Fishers indeed reflect parameters important for their particular computational steps. We further ran experiments on a TRACR-compiled toy model implementing a known ground-truth algorithm and demonstrate that components align with sub-steps of the computation. We also explored a potential application of NPEFF’s parameter perturbation to correcting faulty heuristics used by a model. Finally, we include experiments demonstrating the robustness of NPEFF to choices of hyperparameters.

2 NON-NEGATIVE PER-EXAMPLE FISHER FACTORIZATION (NPEFF)

2.1 FISHER INFORMATION

Consider a classification model $p_\theta(y|\mathbf{x})$ with parameters $\theta \in \mathbb{R}^m$ that maps inputs $\mathbf{x} \in \mathcal{X}$ to a softmax distribution over C labels. Given any example $\mathbf{x} \in \mathcal{X}$, we define the per-example Fisher (PEF) matrix as

$$F(\mathbf{x}) = \mathbb{E}_{y \sim p_\theta(y|\mathbf{x})} \nabla_\theta \log p_\theta(y|\mathbf{x}) \nabla_\theta \log p_\theta(y|\mathbf{x})^T. \quad (1)$$

The Fisher information matrix has an information geometric interpretation as a metric relating local perturbations in parameters to changes in the model’s predictive distribution (Amari, 2016)

$$D_{\text{KL}}(p_\theta(y|\mathbf{x}) \| p_{\theta+\delta}(y|\mathbf{x})) \approx \frac{1}{2} \delta^T F(\mathbf{x}) \delta \quad (2)$$

as $\delta \rightarrow \mathbf{0}$, where D_{KL} is the KL divergence.

If we let $\mathbf{a}_j(\mathbf{x}) = \sqrt{p_\theta(y_j|\mathbf{x})} \nabla_\theta \log p_\theta(y_j|\mathbf{x})$, then we can express the PEF as $F(\mathbf{x}) = \sum_{j=1}^C \mathbf{a}_j(\mathbf{x}) \mathbf{a}_j(\mathbf{x})^T$. We can thus represent the full PEF matrix using only Cm values, which we call its low-rank representation or LRM-PEF. Alternatively, we can use the diagonal of the PEF matrix as its representation, which we call the diagonal PEF or D-PEF (Kirkpatrick et al., 2017). In this case we have

$$\mathbf{f}(\mathbf{x}) = \mathbb{E}_{y \sim p_\theta(y|\mathbf{x})} (\nabla_\theta \log p_\theta(y|\mathbf{x}))^2. \quad (3)$$

Unlike the LRM-PEF which is an exact representation, the D-PEF corresponds to the approximation $F(\mathbf{x}) \approx \text{Diag}(\mathbf{f}(\mathbf{x}))$. Generally, D-PEFs are more tractable to process than LRM-PEFs when the number of classes C is large.

Sparsity Since the number of parameters m can be very large for real world models, storing D-PEFs or LRM-PEFs for a modestly sized data set can become intractable. Fortunately, we empirically observe that most of the entries of the PEFs for typical trained neural networks tend to be very

small in magnitude. This is to be expected from prior works on model pruning (Hoefler et al., 2021), which finds that most parameters are not important for the model’s behavior (Frankle & Carbin, 2018). In our work, we fix some value $K \in \mathbb{N}$ and sparsify each PEF representation by using only the K values with the largest magnitudes. This significantly reduces the amount of required storage and compute with relatively little impact on the accuracy of the representations.

Number of Classes For tasks with only a few classes, we can include the term for every class in equation 1 and equation 3 when computing the PEFs. However, this becomes prohibitively expensive as the number of classes increases, requiring roughly the same amount of computation as required for a backwards pass for each class. For such tasks, we thus discard terms correspond to classes whose probabilities $p_\theta(y|\mathbf{x})$ are below some threshold ϵ .

2.2 DECOMPOSITION

Let $\mathcal{D} = \{\mathbf{x}_1, \dots, \mathbf{x}_n\}$ be a set of examples. Let F_i correspond to our representation of the Fisher matrix for the i -th example, i.e. $F_i = \sum_{j=1}^C \mathbf{a}_j(\mathbf{x}_i)\mathbf{a}_j(\mathbf{x}_i)^T$ if we are using LRM-PEFs or $F_i = \text{Diag}(\mathbf{f}(\mathbf{x}_i))$ for D-PEFs. The decomposition central to NPEFF can be expressed as the non-convex optimization problem

$$\begin{aligned} & \text{minimize} && \sum_{i=1}^n \|F_i - \sum_{j=1}^r W_{ij}H_j\|_F^2 \\ & \text{subject to} && W_{ij} \geq 0, \\ & && H_j \in \mathcal{H}, \end{aligned} \tag{4}$$

where \mathcal{H} corresponds to a subset of $m \times m$ matrices and r is a hyperparameter denoting the number of components to learn. We choose this decomposition since we can interpret the H_j as a “pseudo-Fisher” for the j -th component, and the non-negative coefficients W_{ij} allow us to see the contributions of each component to the KL-divergence of a model’s predictions following a perturbation of its parameters.

For LRM-NPEFF, \mathcal{H} is the set of rank-1 $m \times m$ -positive semi-definite (PSD) matrices. Any element of this \mathcal{H}_j can be expressed as $H_j = \mathbf{g}_j\mathbf{g}_j^T$ for some vector $\mathbf{g}_j \in \mathbb{R}^m$. This decomposition can be described as approximating a set of low-rank PSD matrices as non-negative combinations of a set of shared rank-1 PSD matrices. We present a multi-GPU algorithm performing this decomposition in appendix A. Importantly, this algorithm does not explicitly construct any $m \times m$ -matrix and instead uses a number of inner products between m -dimensional vectors that is independent of m itself.

For D-NPEFF, \mathcal{H} is the set of diagonal $m \times m$ -matrices with non-negative entries. Any element of this \mathcal{H} can be expressed as $H_j = \text{Diag}(\mathbf{h}_j)$ for some non-negative vector $\mathbf{h}_j \in \mathbb{R}_{\geq 0}^m$. Solving equation 4 then reduces to the well-studied problem of non-negative matrix factorization (NMF) (Wang & Zhang, 2012). We used a multi-GPU implementation based on Boureima et al. (2022).

Both variants of NPEFF produce a non-negative matrix $W \in \mathbb{R}_{\geq 0}^{n \times r}$ that we call the coefficient matrix. It defines the relationship between individual examples and components. Each entry W_{ij} represents the contribution of the j -th component to the PEF of the i -th example. The coefficient matrix allows us to get a qualitative understanding of the sub-computation associated to each component. Given a component, we create a list of the examples sorted by the component’s coefficient and look at the ones with the highest coefficients. Those top examples often display an interpretable pattern from which we can infer what processing the component represents.

Both NPEFF variants also produce a collection of m -dimensional vectors that we refer to as the component pseudo-Fishers. Deferring to section 2.3 for further exposition, each component’s pseudo-Fisher vector generates what can be interpreted as an analog of a Fisher information matrix for that component. We express these matrices as $H_j = \mathbf{g}_j\mathbf{g}_j^T$ for an LRM-NPEFF pseudo-Fisher vector $\mathbf{g}_j \in \mathbb{R}^m$. D-NPEFF generates $H_j = \text{Diag}(\mathbf{h}_j)$ for the non-negative pseudo-Fisher vectors $\mathbf{h}_j \in \mathbb{R}_{\geq 0}^m$.

Preprocessing During initial experimentation, we found that using raw PEFs led to components tuned to outlier examples. We suspect that outlier examples tend to have PEFs with large magnitudes, and thus their contributions dominate the loss during optimization. To rectify this, we normalized PEFs to have unit Frobenius norm *before* sparsification. This has the effect of de-emphasizing

examples for which the sparse approximation is poor; however, we expect any difference in the outcome to be minimal. Efficient computation of the Frobenius norm is described in appendix B.

Our decomposition algorithms make use of a dense representation of the pseudo-Fisher vectors, and thus a naive implementation would require the use of rm floats to represent them. However, the sparsification of the PEFs leads to many parameters having few non-zero corresponding entries. We are able to greatly reduce the memory burden by pruning these entries across the PEFs and using a dimensionality of $m' < m$. We suspect these positions do not contain enough effective “data-points” to contribute meaningfully to the factorization, so its validity should be minimally impacted.

Coefficient Fitting Once we have computed the pseudo-Fisher vectors on a data set \mathcal{D} , we can fit a coefficient matrix to PEFs created from another data set \mathcal{D}' . Importantly, this allows us to see if the tunings of NPEFF components generalize to examples not used to generate them. Since both of the LRM-NPEFF and D-NPEFF decomposition algorithms operate by alternating between updating the coefficient matrix and updating the pseudo-Fisher vectors, we can fit coefficients to a fixed set of pseudo-Fishers by repeatedly only performing the coefficient matrix update step. By caching intermediates that do not depend on the coefficients, coefficient fitting can be performed far more efficiently than a full NPEFF decomposition.

Components Set Expansion Having learned an NPEFF decomposition using a large, general set of examples, we can expand the set of components to create components specialized to another set of examples that are of particular interest. The process is similar to that of a regular NPEFF decomposition with the exception that a subset of component pseudo-Fishers are initialized using the existing decomposition. These are then frozen throughout the decomposition procedure. This leads to the frozen components capturing the general-purpose processing trends leaving the non-frozen components to capture processing specific to that set of examples.

2.3 GUIDED PERTURBATIONS

Recall from equation 2 how PEF matrices can be used to relate perturbations of model parameters to changes in its predictive distribution for an example. Using the NPEFF decomposition, we can approximate a PEF matrix for example \mathbf{x}_i as $F_i \approx \alpha_i \sum_{j=1}^r W_{ij} H_j$, where α_i is the Frobenius norm of F_i . Plugging this into equation 2 gives us

$$D_{\text{KL}}(p_{\theta}(y|\mathbf{x}_i) || p_{\theta+\delta}(y|\mathbf{x}_i)) \approx \frac{\alpha_i}{2} \sum_{j=1}^r W_{ij} \delta^T H_j \delta \quad (5)$$

for a parameter perturbation $\delta \in \mathbb{R}^m$. From this, our choice of calling H_j the “pseudo-Fisher matrix” for the j -component should be clear: it can be used to relate the disruption of the model’s predictions on examples utilizing the component to perturbations of parameters. Furthermore, this justifies our choice of decomposition method since the uncovered factors can be readily interpreted in equation 5.

The equation equation 5 provides a theoretically principled way to verify relationship between parameters and examples uncovered by NPEFF. The goal is to find a perturbation $\delta \in \mathbb{R}^m$ such that $\delta^T H_k \delta$ is large when $k = j$ for a chosen component j and is small otherwise. Once one is found, we can compare the KL-divergences between the perturbed and original models’ predictions on examples to their coefficients for the j -th component.

For LRM-NPEFF, recall that each pseudo-Fisher matrix H_k can be expressed as $\mathbf{g}_k \mathbf{g}_k^T$ for some vector $\mathbf{g}_k \in \mathbb{R}^m$. Thus $\delta^T H_k \delta = (\mathbf{g}_k^T \delta)^2$. We wish to find a $\delta \in \mathbb{R}^m$ such that $\mathbf{g}_k^T \delta$ has a large magnitude for $k = j$ and small magnitude otherwise. We found that simply using $\delta \propto \pm \mathbf{g}_j$ performed well, but the selectivity of the perturbation could be improved by taking the orthogonal rejection of $\pm \mathbf{g}_j$ onto a subset of the other components’ pseudo-Fishers. Namely, we orthogonally reject $\pm \mathbf{g}_j$ onto \mathbf{g}_k if the magnitude of their cosine-similarities is below some threshold. The threshold is used to prevent similar components from interfering in the construction of the perturbation. We found a threshold of 0.35 to work well, which is what we used throughout our experiments. The construction of the perturbation for D-NPEFF is more involved and is presented in appendix C.

3 EXPERIMENTS

3.1 COMPONENT TUNINGS AND PERTURBATIONS

We ran LRM-NPEFF on two NLP models and ran D-NPEFF on a vision model. The NLP models were BERT-base fine-tuned on MNLI and QQP, respectively (Devlin et al., 2018). QQP is a binary classification task that aims to determine whether a pair of questions are duplicates of each other (Wang et al., 2018a). MNLI is a natural language inference (NLI) task that involves determining whether a given hypothesis is implied by, contradicted by, or neutral with respect to a given hypothesis (Williams et al., 2018). Thus, it has three classes. For the vision model, we used a ResNet-50 (He et al., 2016) trained on the ImageNet classification task (Russakovsky et al., 2015). ImageNet involves classifying an image as one of 1000 fine-grained classes.

When learning the NPEFF components for QQP, we used 50k examples heldout from the canonical train split to produce PEFs. For the NLI model, we used 50k examples from the SNLI data set (Bowman et al., 2015). Like the MNLI data set used to train the model, SNLI is also an NLI task with the main difference being that SNLI examples come from a single domain while MNLI has examples from multiple domains. We chose to do this to get a better idea of how NPEFF uncovers heuristics when a model generalizes to new data sets. We used 20k examples from the train split of ImageNet 2012 to produce PEFs for the vision model. We ignored classes with a probability of less than $3e-3$ when computing the PEFs for the vision model.

We used 512 components when running NPEFF on the NLI and vision models, and we used 256 components for the QQP model. Once the NPEFF pseudo-Fishers were computed, we fit coefficients to PEFs from a heldout set of examples for each model. We used 50k SNLI examples for the NLI model, 40,430 examples from the QQP validation set for the QQP model, and 30k examples from the ImageNet validation set for the vision model. All of the component tunings and perturbations presented in this section are from these heldout sets. More details on the models and data sets used can be found in see appendix D. There, we also go into detail about the hyperparameters used when computing the PEFs and running NPEFF for these experiments.

3.1.1 COMPONENT TUNINGS

COMPONENT 70: Which is the best dish tv connection in hyderabad ? Which is the best dish tv connection in bangalore ? Which is the best eye hospital in kolkata ? Which is the best eye hospital in pune ? Where can i buy second hand books in hyderabad ? Where can i buy second hand books in india ? What is the best coaching center for gre in chennai ? What is the best coaching center for gre in bangalore ?	COMPONENT 345: [P] Two men in the kitchen with a pot on the stove. [H] Two men cook a pot of soup in the kitchen. [P] A young girl is eating as she sits at a table full of food. [H] A young girl is eating fruit at a table. [P] A child is looking at an exhibit . [H] A child looks at an exhibit of a monkey . [P] 3 men are working on a boat . [H] 3 men are working on a crab boat in alaska .
---	---

Figure 1: Top examples for two language components. The examples presented are the ones with the 4 highest coefficients. **(Left)** QQP component. The model correctly predicts that these questions pairs are not duplicates. Despite asking for the same information, they differ in geographic location. **(Right)** The model correctly predicted “neutral” for these examples. The hypothesis is consistent with the premise but includes additional information that cannot be inferred from the premise.

For all models, we found that most components appeared to have some potential interpretable tuning. We present the top examples of some components in fig. 1 for the NLP models and fig. 2 for the vision model. More examples of tuned component top examples are provided in appendix J.

Some components for the NLP models appeared to be tuned to strategies of solving their respective tasks for specific types of examples. These were typically selective for one of the predictions, and the top examples all contained some common task-specific group of features. Other components appeared to be tuned for features not directly related to the task (e.g. existence of certain kinds of words). It was often the case that a component would use a combination of these two tuning styles.

Many components for the vision model had tunings that included relatively low-level features such as color, shape, and spatial patterns. More abstract, high-level features also played in a role in the tunings of many components. These range from broad, coarse-grained attributes such as the

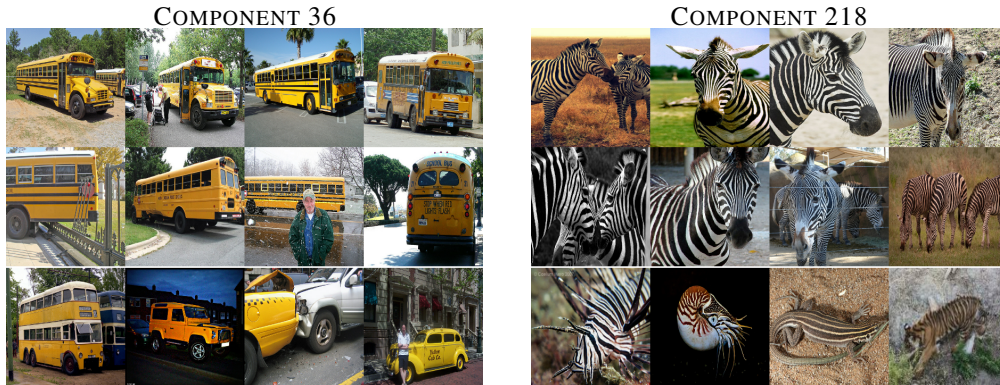


Figure 2: Top examples for two vision components. The top two rows for each component are the examples with the 8 highest coefficients. The bottom row for each component contains selected examples from the set of top 32 examples. **(Left)** The examples with the highest coefficients are all school buses. In general, examples with high coefficients have a yellow vehicle in them. **(Right)** The examples with the highest coefficients are all zebras. In general, examples with high coefficients have a striped animal in them. The specific type of animal does not seem important with fish, mollusks, lizards, and mammals being included.

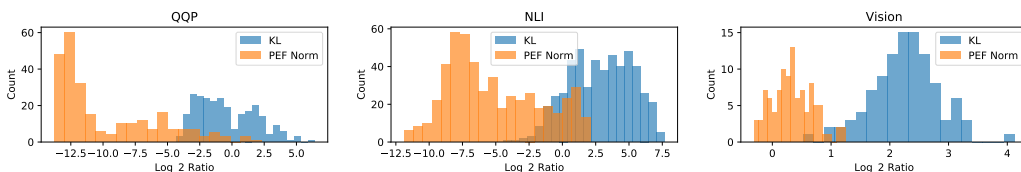


Figure 3: Histograms of the \log_2 ratios between top component examples and random examples for KL-divergence and PEF norm.

general category of the image subject (e.g. animal, plant, vehicle, architecture, technology, etc.) to more specific, fine-grained attributes such as the fur patterns of dogs. Many of the components had tunings that included both low-level and high-level features. In those cases, the low-level features were often predictive of the higher level ones.

3.1.2 PERTURBATIONS

For the LRM-NPEFF experiments on the NLI and QQP models, we used the perturbation method discussed in section 2.3. Perturbation vectors were scaled to have an L2 norm of 0.1 before applying them to the model parameters. We then measured the per-example KL-divergence of the perturbed model’s predictions from the original model’s predictions. To score the selectivity of the perturbation’s impact on the top examples of a component, we calculated the ratio of the average of this KL-divergence for the component’s top 128 examples to the average KL-divergence for a random subset of 10k examples. Since the sign of the perturbation is not determined by the method in section 2.3, we try both adding and subtracting the perturbation to the model parameters. The reported scores correspond to whichever has a higher KL-ratio. Details of the perturbation experiments for the D-NPEFF decomposition of the vision model can be found in appendix E.

Looking at the expression equation 5 relating the KL-divergence of a model’s prediction to a perturbation of its parameters, we see that the KL-divergence is directly proportional to norm of the example’s PEF. In contrast, the coefficients used to rank the top examples for a component are computed using normalized PEFs and thus are independent of their norms. To explore the impact of this confounding factor, we computed the ratio of the average PEF Frobenius norm of the top 128 examples for each component to the average norm of a random subset of 10k examples.

Histograms of the KL-divergence and PEF norm ratios are presented in fig. 3. For all models, these histograms clearly show that the KL-divergence ratios tended to be significantly higher than the PEF

norm ratios. This supports our claim that the directions in parameter space uncovered by NPEFF are specifically important for their respective component top examples. Furthermore, this helps verify that the concepts and heuristics uncovered by NPEFF correspond to actual processing methods used by the model.

3.2 TOY MODEL WITH KNOWN GROUND TRUTH

Since it is difficult to evaluate whether a method uncovers concepts actually used by a real-world model, we ran experiments using a synthetic task and transformer model compiled by TRACR (Lindner et al., 2023) that implements a RASP program (Weiss et al., 2021). This task simulates an extremely simplified NLI task. An example looks like [BOS] Q1 S1 O1 Q2 S2 O2, which is a concatenation of a premise and hypothesis. The Q1, Q2 tokens correspond to All or Some, and a Q S O segment can be thought of as the sentence [All/Some] [subject] [verb] [object]. The verb is assumed fixed and shared between the premise and hypothesis, so it is not explicitly represented. Subjects and objects are chosen from the same set of options containing a hierarchical structure so that we can have a `is_a_subtype_of` relation between options. Each example is given a label of `entails` or `neutral`. Appendix H contains the RASP program solving this task. It is compiled by TRACR to an encoder-style Transformer (Vaswani et al., 2017) with 4 attention heads, a model dimension of 25, feedforward hidden dimension of 1320, and 23 layers with 23.5M params. Its output at the final sequence position forms the prediction for the example.

We ran LRM-NPEFF on 1616 examples using either 32 or 128 components. Since we know how the model processes examples, we can programmatically search for components whose top examples all contain a concept used by the model. We found that 30/32 and 92/128 components had 128 top examples all containing at least one concept. See appendix H for details on this programmatic search along with a detailed breakdown of component tunings. Although caution should be used when extending these results to real-world models since organic processing might differ from TRACR’s implementations, these results demonstrate that NPEFF is able to extract concepts actually used by a model in this setting.

3.3 HYPERPARAMETER EXPLORATION

We explored the impact of various choices of hyperparameters on the LRM-NPEFF decomposition. The NLI model’s LRM-NPEFF from section 3.1 was used as the baseline setting. To concisely compare component tunings, we used the cosine similarity of component coefficient vectors. Components with a high cosine similarity tended to have similar top examples.

Sparsity We ran LRM-NPEFF keeping the top 16384, 65536, and 262144 values per PEF. We used 20k examples and 128 components. Given a pair of runs, we looked at each component from one of the runs and recorded its max cosine similarity with any component from the other run. If this value is high for most components in both directions for a pair of runs, then most of the concepts from one run have an analogous concept in the other. This metric had an average value of 0.77 when comparing the components from the 16384-value run against either of the other runs. The 65536-value run had an average of value of 0.76 and 0.80 when compared against 16384-value and 262144-value runs. The 262144-value run had an average of value of 0.77 and 0.80 when compared against 16384-value and 65536-value runs. Hence the sets of learned components tended to be fairly similar with no major qualitative difference being observed between their tunings. Information about how well the PEFs were approximated at different levels of sparsity can be found in appendix G.

Number of Components We ran LRM-NPEFF using 32, 128, and 512 components. To compare a pair of runs A and B, suppose that run B has more components than run A. For each component i of run A, we found the subset of run B’s components whose coefficient cosine similarity to that component i was greater than to any other of run A’s components. For all pairs of runs, we found that every component from the smaller run had at least one corresponding component from the larger run. Qualitatively, we found that the groups of components from the larger run corresponding to each component from the smaller run had similar tunings. More precisely, these groups tended to be more fine-grained “splits” of the component from the smaller run. For example, a component

tuned to hypotheses containing a word that contradicts a word in the premise might have a split where the relevant words are colors and another split where they are “cat” and “dog”.

Number of Steps To explore the convergence of the coefficient matrix as the NPEFF learning algorithm progresses, we performed the decomposition for 1500 steps and saved the matrix every 50 steps. A graph of the average component coefficient cosine similarity with its final value across steps can be found in fig. 5. Notably, the average similarity exceeded 95% by 700 steps and 99% by 1100 steps.

D-NPEFF vs. LRM-NPEFF We repeated the experiments of section 3.1 for the NLI and vision model but using D-NPEFF instead of LRM-NPEFF and vice-versa. For the NLI model, we found D-NPEFF to generate fewer components with readily interpretable tunings than LRM-NPEFF. While most of the LRM-NPEFF components appeared tuned, only about half of the D-NPEFF components appeared tuned. Furthermore, the perturbation of D-NPEFF components led to less selective changes in model predictions than for the LRM-NPEFF components with a median KL-ratio of 5.26 compared to 7.64. However, this might just be an artifact of the difference between the perturbation methods of the two flavors of NPEFF.

The LRM-NPEFF results on the vision model were far worse than the D-NPEFF results. Far fewer components had interpretable tunings, and top examples of tuned components were significantly noisier. The selectivity of perturbations of the LRM-NPEFF components was also lower than for the D-NPEFF components with a median KL ratio of 2.45 compared to 4.81. We suspect that using a fixed number of non-zero entries led to examples with high rank PEFs having poor sparse approximations. Left to future work, possible methods to adapt LRM-NPEFF to tasks with many classes (and thus potentially high rank PEFs) include varying the number of kept entries with PEF rank and using a different low-rank approximation to the PEF instead of just using a subset of classes.

3.4 COMPARISON TO EXISTING INTERPRETABILITY METHODS

While there are no existing unsupervised concept discovery algorithms directly comparable to NPEFF, we can adapt the methods of Ghorbani et al. (2019) to be a baseline. Ghorbani et al. (2019) learns concepts through k-means clustering of activation space representations of image segments. We compared NPEFF to a more generalized version of this operating directly on examples rather than image segments, which allowed us to run experiments on text tasks. We used the distance of an example’s activations from its cluster’s centroid to rank examples within a cluster.

We ran this baseline for both the NLI and vision models. We used the encoder’s final representation of the CLS token as the activations for the NLI model. For the vision model, we used the output of the global average pooling layer that immediately precedes the classification layer. Using the same sets of examples as in section 3.1, we learned 128 clusters for each model. Most of the top examples for the clusters displayed some human-interpretable tuning as ascertained through examination of their top examples. Top examples of some clusters are presented in appendix M. We used TCAV (Kim et al., 2018) to test whether a relationship existed between the top examples for a cluster/component and the prediction of at least one class for the NLI model. We found a statistically significant relationship existed for every k-means cluster and every LRM-NPEFF component. Details can be found in appendix I.

Qualitatively, we found some similarities in the tunings of NPEFF and baseline components with NPEFF producing a more diverse set of tunings. To get a more quantitative comparison, we used the average max cosine-similarity metric from section 3.3 to compare tunings. Here, we used a vector of 0s and 1s indicating cluster membership as the “coefficients vector” for a k-means cluster. For the NLI model, we found that k-means clusters had an average max cosine similarity of 0.20 against the NPEFF components and a value of 0.19 in the opposite direction. Since NPEFF coefficients and cluster “coefficients” represent different types of quantities, we should note that this metric provides a cruder similarity measure than when comparing between NPEFF components.

Nevertheless, we would expect differences in recovered concepts. The differences in recovered concepts highlights several advantages of NPEFF. The k-means baseline operates on activations from a single layer near the output of the model while NPEFF operates on PEFs containing information from the entire model. Hence NPEFF can pinpoint what part of the model performs certain com-

putations. In contrast, a full-model decomposition over activations becomes tricky when the total activation space does not have fixed dimension (e.g. the variable sequence length of transformers). The ability to make informed modifications to parameters to directly test whether the model actually uses a recovered concept is a further advantage unique to NPEFF.

3.5 EXAMPLE APPLICATION: FIXING FLAWED HEURISTICS

We experimented using NPEFF with the NLI model to see what heuristics it uses when it makes incorrect predictions. To do so, we created a filtered set of PEFs corresponding to examples on which the model made an incorrect prediction. We then performed the components set expansion procedure to learn 64 components specialized to these examples. Finally, we fit coefficients to a non-filtered set of examples using the expanded NPEFFs. See appendix F for details on this process.

The components in the expansion were more likely to have a high fraction of incorrect predictions in their top examples. More precisely, 41% of the expanded components had incorrect predictions for at least 50% of their top 16 examples compared to just 4.3% of the original components. Such components could generally be placed into one of three groups: correct heuristics with inconsistent labeling, completely wrong heuristics, or flawed heuristics. Since LRM-NPEFF connects components to directions in parameter space through their pseudo-Fishers, we can try to alter the model parameters to selectively fix components tuned to incorrect heuristics. We selected the subset of expanded components whose top 16 examples contained at least 8 incorrect predictions. The top examples of some these components are provided in appendix L. We then performed perturbations on these components using a similar methodology to section 3.1.2 but with a larger perturbation magnitude of $3e-1$. Out of the 48 components deemed to correspond to incorrect heuristics, we found four components that increased the model’s accuracy by at least 0.5% after being perturbed. While these results are promising, we emphasize that this method of fixing faulty heuristics using NPEFF is mostly a proof of concept. We leave improvements to this method such as incorporating loss gradient information to future work.

4 RELATED WORK

Methods reliant on ranking or grouping examples are common in the interpretability literature. For example, the activation value of a single neuron is a frequently used metric to derive such rankings (Sajjad et al., 2022; Bolukbasi et al., 2021; Bau et al., 2017; Szegedy et al., 2013). Alternate methods include using agglomerative clustering on token-level BERT representations to find groups of representations corresponding to concepts (Dalvi et al., 2022), using supervised probing task to learn latent interpretable representations (Michael et al., 2020), and unsupervisedly finding interpretable directions in the latent space of a generative adversarial network (Voynov & Babenko, 2020).

Kim et al. (2018) uses user-defined groups of examples to represent an abstract concept. Ghorbani et al. (2019) uses clustering of activation space representations of image segments to automatically learn concepts. Yeh et al. (2020) learns concepts by projecting activations at a given layer onto a set of learned vectors, setting the dot products below a threshold to zero, and then using a learned mapping back to activation space before being processed by the rest of the network. They add regularizers to encourage concepts to be coherent and unique.

Representing a neural network as a set of sub-computations underlies some vision interpretability work. Zhang et al. (2018) learns an explanatory graph given a convolutional neural network. They create nodes corresponding to disentangled convolutional filters and assign edges based on the relative spatial displacement of node activations between neighboring layers. For each example, Wang et al. (2018b) learns a scalar control gate for each channel in each layer of a convolutional network. They are fit using a loss that encourages the gates to be as sparse as possible while preserving the model’s predictions on the example. Clustering of these per-example routing maps produces clusters that reflect input layout patterns.

5 CONCLUSION

NPEFF presents a novel direction in model interpretability research. Applicable to any model with differentiable parameters, it automatically discovers concepts and heuristics used by a model.

NPEFF further grounds these in the model’s parameter space and allows for their selective perturbations. In addition to being useful in verifying that these concepts and heuristics faithfully represent the model’s processing, it opens up the possibility of modifying the model informed by this knowledge. In future work, we hope to further develop some of the applications of NPEFF explored in this paper as well as explore its viability in facilitating scientific discovery.

REFERENCES

- Martín Abadi, Paul Barham, Jianmin Chen, Zhifeng Chen, Andy Davis, Jeffrey Dean, Matthieu Devin, Sanjay Ghemawat, Geoffrey Irving, Michael Isard, et al. {TensorFlow}: a system for {Large-Scale} machine learning. In *12th USENIX symposium on operating systems design and implementation (OSDI 16)*, pp. 265–283, 2016.
- Shun-ichi Amari. *Information geometry and its applications*, volume 194. Springer, 2016.
- David Bau, Bolei Zhou, Aditya Khosla, Aude Oliva, and Antonio Torralba. Network dissection: Quantifying interpretability of deep visual representations. In *Proceedings of the IEEE conference on computer vision and pattern recognition*, pp. 6541–6549, 2017.
- Tolga Bolukbasi, Adam Pearce, Ann Yuan, Andy Coenen, Emily Reif, Fernanda Viégas, and Martin Wattenberg. An interpretability illusion for bert. *arXiv preprint arXiv:2104.07143*, 2021.
- Ismael Boureima, Manish Bhattarai, Maksim Eren, Erik Skau, Philip Romero, Stephan Eidenbenz, and Boian Alexandrov. Distributed out-of-memory nmf of dense and sparse data on cpu/gpu architectures with automatic model selection for exascale data. *arXiv preprint arXiv:2202.09518*, 2022.
- Samuel R Bowman, Gabor Angeli, Christopher Potts, and Christopher D Manning. A large annotated corpus for learning natural language inference. *arXiv preprint arXiv:1508.05326*, 2015.
- Juan José Burred. Detailed derivation of multiplicative update rules for nmf. *Paris, France*, 2014.
- Piotr Dabkowski and Yarin Gal. Real time image saliency for black box classifiers. *Advances in neural information processing systems*, 30, 2017.
- Fahim Dalvi, Abdul Rafae Khan, Firoj Alam, Nadir Durrani, Jia Xu, and Hassan Sajjad. Discovering latent concepts learned in bert. *arXiv preprint arXiv:2205.07237*, 2022.
- Jacob Devlin, Ming-Wei Chang, Kenton Lee, and Kristina Toutanova. Bert: Pre-training of deep bidirectional transformers for language understanding. *arXiv preprint arXiv:1810.04805*, 2018.
- Jonathan Frankle and Michael Carbin. The lottery ticket hypothesis: Finding sparse, trainable neural networks. *arXiv preprint arXiv:1803.03635*, 2018.
- Amirata Ghorbani, James Wexler, James Y Zou, and Been Kim. Towards automatic concept-based explanations. *Advances in Neural Information Processing Systems*, 32, 2019.
- Kaiming He, Xiangyu Zhang, Shaoqing Ren, and Jian Sun. Deep residual learning for image recognition. In *Proceedings of the IEEE conference on computer vision and pattern recognition*, pp. 770–778, 2016.
- Torsten Hoefler, Dan Alistarh, Tal Ben-Nun, Nikoli Dryden, and Alexandra Peste. Sparsity in deep learning: Pruning and growth for efficient inference and training in neural networks. *J. Mach. Learn. Res.*, 22(241):1–124, 2021.
- Been Kim, Martin Wattenberg, Justin Gilmer, Carrie Cai, James Wexler, Fernanda Viegas, et al. Interpretability beyond feature attribution: Quantitative testing with concept activation vectors (tcav). In *International conference on machine learning*, pp. 2668–2677. PMLR, 2018.
- Diederik P Kingma and Jimmy Ba. Adam: A method for stochastic optimization. *arXiv preprint arXiv:1412.6980*, 2014.

-
- James Kirkpatrick, Razvan Pascanu, Neil Rabinowitz, Joel Veness, Guillaume Desjardins, Andrei A Rusu, Kieran Milan, John Quan, Tiago Ramalho, Agnieszka Grabska-Barwinska, et al. Overcoming catastrophic forgetting in neural networks. *Proceedings of the national academy of sciences*, 114(13):3521–3526, 2017.
- Daniel D Lee and H Sebastian Seung. Learning the parts of objects by non-negative matrix factorization. *Nature*, 401(6755):788–791, 1999.
- Xuhong Li, Haoyi Xiong, Xingjian Li, Xuanyu Wu, Xiao Zhang, Ji Liu, Jiang Bian, and Dejing Dou. Interpretable deep learning: Interpretation, interpretability, trustworthiness, and beyond. *Knowledge and Information Systems*, 64(12):3197–3234, 2022.
- David Lindner, János Kramár, Matthew Rahtz, Thomas McGrath, and Vladimir Mikulik. Tracr: Compiled transformers as a laboratory for interpretability. *arXiv preprint arXiv:2301.05062*, 2023.
- Michael Matena and Colin Raffel. Merging models with fisher-weighted averaging. *arXiv preprint arXiv:2111.09832*, 2021.
- R Thomas McCoy, Junghyun Min, and Tal Linzen. Berts of a feather do not generalize together: Large variability in generalization across models with similar test set performance. *arXiv preprint arXiv:1911.02969*, 2019.
- Julian Michael, Jan A Botha, and Ian Tenney. Asking without telling: Exploring latent ontologies in contextual representations. *arXiv preprint arXiv:2004.14513*, 2020.
- Olga Russakovsky, Jia Deng, Hao Su, Jonathan Krause, Sanjeev Satheesh, Sean Ma, Zhiheng Huang, Andrej Karpathy, Aditya Khosla, Michael Bernstein, Alexander C. Berg, and Li Fei-Fei. ImageNet Large Scale Visual Recognition Challenge. *International Journal of Computer Vision (IJCV)*, 115(3):211–252, 2015. doi: 10.1007/s11263-015-0816-y.
- Hassan Sajjad, Nadir Durrani, and Fahim Dalvi. Neuron-level interpretation of deep nlp models: A survey. *Transactions of the Association for Computational Linguistics*, 10:1285–1303, 2022.
- Daniel Smilkov, Nikhil Thorat, Been Kim, Fernanda Viégas, and Martin Wattenberg. Smoothgrad: removing noise by adding noise. *arXiv preprint arXiv:1706.03825*, 2017.
- Mukund Sundararajan, Ankur Taly, and Qiqi Yan. Axiomatic attribution for deep networks. In *International conference on machine learning*, pp. 3319–3328. PMLR, 2017.
- Christian Szegedy, Wojciech Zaremba, Ilya Sutskever, Joan Bruna, Dumitru Erhan, Ian Goodfellow, and Rob Fergus. Intriguing properties of neural networks. *arXiv preprint arXiv:1312.6199*, 2013.
- Ashish Vaswani, Noam Shazeer, Niki Parmar, Jakob Uszkoreit, Llion Jones, Aidan N Gomez, Łukasz Kaiser, and Illia Polosukhin. Attention is all you need. *Advances in neural information processing systems*, 30, 2017.
- Andrey Voynov and Artem Babenko. Unsupervised discovery of interpretable directions in the gan latent space. In *International conference on machine learning*, pp. 9786–9796. PMLR, 2020.
- Alex Wang, Amanpreet Singh, Julian Michael, Felix Hill, Omer Levy, and Samuel R Bowman. Glue: A multi-task benchmark and analysis platform for natural language understanding. *arXiv preprint arXiv:1804.07461*, 2018a.
- Yu-Xiong Wang and Yu-Jin Zhang. Nonnegative matrix factorization: A comprehensive review. *IEEE Transactions on knowledge and data engineering*, 25(6):1336–1353, 2012.
- Yulong Wang, Hang Su, Bo Zhang, and Xiaolin Hu. Interpret neural networks by identifying critical data routing paths. In *proceedings of the IEEE conference on computer vision and pattern recognition*, pp. 8906–8914, 2018b.
- Gail Weiss, Yoav Goldberg, and Eran Yahav. Thinking like transformers. In *International Conference on Machine Learning*, pp. 11080–11090. PMLR, 2021.

-
- Adina Williams, Nikita Nangia, and Samuel Bowman. A broad-coverage challenge corpus for sentence understanding through inference. In *Proceedings of the 2018 Conference of the North American Chapter of the Association for Computational Linguistics: Human Language Technologies, Volume 1 (Long Papers)*, pp. 1112–1122. Association for Computational Linguistics, 2018. URL <http://aclweb.org/anthology/N18-1101>.
- Thomas Wolf, Lysandre Debut, Victor Sanh, Julien Chaumond, Clement Delangue, Anthony Moi, Pierric Cistac, Tim Rault, Rémi Louf, Morgan Funtowicz, et al. Huggingface’s transformers: State-of-the-art natural language processing. *arXiv preprint arXiv:1910.03771*, 2019.
- Chih-Kuan Yeh, Been Kim, Sercan Arik, Chun-Liang Li, Tomas Pfister, and Pradeep Ravikumar. On completeness-aware concept-based explanations in deep neural networks. *Advances in neural information processing systems*, 33:20554–20565, 2020.
- Quanshi Zhang, Ruiming Cao, Feng Shi, Ying Nian Wu, and Song-Chun Zhu. Interpreting cnn knowledge via an explanatory graph. In *Proceedings of the AAAI conference on artificial intelligence*, volume 32, 2018.

A LRM-NPEFF DECOMPOSITION ALGORITHM

Let $\mathcal{D} = \{\mathbf{x}_1, \dots, \mathbf{x}_n\}$ be a set of examples. Let us represent the set of LRM-PEFs via the rank-3 tensor $A \in \mathbb{R}^{n \times c \times m}$, where n is the number of examples, c is the number of classes, and m is the number of parameters. The Fisher information matrix for the i -th example can be expressed as $A_i^T A_i$, where $A_i \in \mathbb{R}^{c \times m}$. While our implementation can handle using a different rank for each PEF (i.e. the number of rows of A_i varying with i), we assume a constant rank here for ease of presentation. The decomposition equation 4 becomes learning matrices $W \in \mathbb{R}^{n \times r}$ and $G \in \mathbb{R}^{r \times m}$ such that

$$\begin{aligned} & \text{minimize} && \sum_{i=1}^n \|F_i - \sum_{j=1}^r W_{ij} \mathbf{g}_j \mathbf{g}_j^T\|_F^2 \\ & \text{subject to} && W_{ij} \geq 0, \end{aligned} \tag{6}$$

where \mathbf{g}_j denotes the j -th row of G .

To solve equation 6, we take a coordinate descent approach reminiscent of the multiplicative update algorithm for NMF where we alternate between updating the W and G matrices (Lee & Seung, 1999). Our W -update step is essentially a the W -update step from the multiplicative update NMF algorithm. For the G -update step, we perform a gradient descent step with a fixed learning rate. It is possible to perform both steps without having to explicitly construct and $m \times m$ -matrices and instead only perform inner products between m -dimensional vectors. The number of such inner products used in the algorithm is independent of m . We go over how to efficiently perform these steps and split the work amongst multiple GPUs in the following.

A.1 W-UPDATE STEP

Recall that the multiplicative update step in NMF involves computing non-negative numerator and denominator matrices $N, D \in \mathbb{R}^{n \times r}$. The matrix W is then updated via the element-wise rule $W_{ij} \mapsto W_{ij} N_{ij} / D_{ij}$.

Computing the numerator starts with computing the rank-3 tensor $B \in \mathbb{R}^{n \times c \times r}$ with elements given by $B_{ijk} = \sum_{\ell=1}^m A_{ij\ell} G_{k\ell}$. The numerator is then given element-wise by $N_{ik} = \sum_{j=1}^c B_{ijk}^2$. The denominator is then given by $D = W((GG^T) \odot (GG^T))$, where \odot denotes the Hadamard product.

A.2 G-UPDATE STEP

The gradient of the loss with respect to G consists of two terms $T_1, T_2 \in \mathbb{R}^{r \times m}$ that are added together. The first term is given by $T_1 = 4((W^T W) \odot (GG^T))G$. Computation of the second term starts by computing the rank-3 tensor $B \in \mathbb{R}^{n \times c \times r}$ as was done for the W -update step. The second term is then obtained element-wise as $[T_2]_{i\ell} = -4 \sum_{j=1}^n \sum_{k=1}^c W_{ji} \beta_{jki} A_{jkl}$.

A.3 MULTI-GPU IMPLEMENTATION DETAILS

Our strategy for distributing work across multiple GPUs is similar to that of Boureima et al. (2022). We partition the last axis of the A tensor and columns of G across the GPUs. The W matrix is replicated across all GPUs. Two all-reduces are needed per step: when computing B and when computing GG^T . If doing a G -update step immediately after a W -update step, we can cache copies of these matrices during the W -update step and use them for the G -update step.

A.4 OTHER CONSIDERATIONS

We initialized W using the uniform distribution on $[0, 1]$. We initialized G using a normal distribution with zero mean and standard deviation of $\sqrt{2}/\sqrt{rm}$. Since the PEFs were normalized to roughly unit L2 norm, we chose this scaling so that the initial reconstructions would also have roughly unit L2 norms as well.

After initialization, we found it crucial to freeze W and only train G for a bit before commencing joint training. This is because if the G is a poor fit for the W , the W update step will end up setting W to zero. Since the W update is multiplicative, it remains zero throughout the remainder of training if this happens. We suspect that this behavior can be explained due to the nature of the multiplicative update step. It can be shown that the multiplicative update step is equivalent to gradient descent with

a variable element-wise learning rate (Burred, 2014). Unlike traditional gradient descent that uses a small gradient step, the variable learning can become large. This makes it possible for the W to jump directly to zero or some similarly small value. If the loss is greater than the Frobenius norm of the PEFs, then setting W to zero will result in a lower loss. Hence, jumping to zero can decrease the loss in such cases.

A.5 CONVERGENCE

While we do not provide a proof of convergence of our LRM-NPEFF decomposition algorithm, we can make a heuristic argument for its convergence. Following the proof of convergence for regular multiplicative-update NMF (Lee & Seung, 1999), we can show that the loss will be non-increasing following the W -update step. For a sufficiently small step size, we can expect the gradient descent step from the G -update to not increase the loss as well. Since the loss is bounded from below by 0, it follows that the loss should eventually converge. When actually running LRM-NPEFF, we found the loss to be non-increasing with the rate of decrease decelerating as the number of steps increased.

A.6 RUN TIME AND SCALING INFORMATION

Typically, our LRM-NPEFF decomposition took between 1 to 8 hours depending on the problem size and number of GPUs used. We used a server with 4x A6000 GPUs; however, we often did not use all of the GPUs. Using the same set up as the NLI model in section 3.1, we report times per joint update step (i.e. a W -update followed by a G update) here. For a 512 component decomposition, we had a step time of 29156 ms on 2 GPUs and 15022 ms on 4 GPUs. For a 128 component decomposition, we had a step time of 14388 ms on 1 GPU and 6975 ms on 2 GPUs. For a 32 component decomposition, we had a step time of 3190 ms on 1 GPU and 1530 ms on 2 GPUs. Thus our implementation obtains a near linear speed up with increasing the number of GPUs.

B COMPUTATION OF LRM-PEF FROBENIUS NORM

Let us represent the PEF $F \in \mathbb{R}^{m \times m}$ of an example as an LRM-PEF $A^T A$, where $A \in \mathbb{R}^{c \times m}$. Using properties of the Frobenius norm, we see that

$$\|F\|_F = \|A^T A\|_F = \|AA^T\|_F. \quad (7)$$

Since AA^T only has c^2 elements, its Frobenius norm can easily be evaluated.

C D-NPEFF PERTURBATION METHOD

We make use of a method based on the Fisher-weighted parameter averaging (FWPA) introduced by Matena & Raffel (2021) to construct a perturbation to selectively disrupt the processing represented by a D-NPEFF component. Let $\theta \in \mathbb{R}^m$ denote the parameters of the original model. Let $\mathbf{f} \in \mathbb{R}^m$ denote the diagonal of the Fisher information matrix of the original model over the entire data set. This is simply the expectation of the diagonal PEFs with respect to the data distribution. Let $\mathbf{h} \in \mathbb{R}^m$ denote the pseudo-Fisher of the component we wish to perturb. Our FWPA-based perturbation method takes in the following hyperparameters: perturbation magnitude $\delta > 0$, merging coefficient $\lambda \in [0, 1]$, and sign-pattern $\mathbf{s} \in \{-1, 1\}^m$ (discussed in the following paragraphs). The parameters $\phi \in \mathbb{R}^m$ of the perturbed model are provided element-wise by

$$\phi_i = \frac{(1 - \lambda)f_i\theta_i + \lambda h_i(\theta_i + s_i\delta)}{(1 - \lambda)f_i + \lambda h_i}, \quad (8)$$

where we default to having $\phi_i = \theta_i$ when both f_i, h_i are approximately zero. This can be interpreted as the Fisher-weighted merge of the original model with a corrupted version where each parameter has been shifted by a magnitude of δ . Intuitively, we expect the perturbed parameters to be closer to their original values when they are more important to the original model’s behavior and farther away when more important for the given component. This has the effect of selectively altering the model’s predictions for examples for which it uses the component’s corresponding sub-computation.

Sign Pattern The need for the sign pattern hyperparameter arises from the fact that the expression predicting the KL-divergence between perturbed and original predictions depends only on the element-wise square of the perturbation. Different choices of the sign pattern will result in different distributions over classes that all should have the same KL-divergence with the original predictive distribution. The invariance of the KL-divergences to the choice of sign pattern, however, can break down when we consider the finite perturbations used in practice instead of the infinitesimal perturbations of the theory.

We use a heuristic method for choosing the sign pattern. First, we assume that we have some set of examples $\mathcal{D}_p = \{\mathbf{x}_1, \dots, \mathbf{x}_\ell\}$ whose predictions we wish to selectively perturb. This will typically be the top examples for a component. For each parameter, we want to move in the direction that increases the KL-divergence of the model’s predictions on these examples the most. Hence, we use a sign vector given element-wise by

$$s_i = \text{sign} \frac{\partial}{\partial \theta_i} \sum_{j=1}^{\ell} D_{\text{KL}}(\text{sg}[p_{\theta}(y|\mathbf{x}_j)] \| p_{\theta}(y|\mathbf{x}_j)), \quad (9)$$

where the `sg` is the stop-gradient operator.

Other Hyperparameters Once we have chosen a sign pattern, we then find hyperparameters δ, λ such that the average KL-divergence for the chosen examples \mathcal{D}_p fell in a predetermined range. We accomplished this via a randomized search heuristic.

Recall that our goal is to find values $\delta > 0$ and $\lambda \in [0, 1]$ such that the average KL-divergence of the perturbed model’s predictions belongs to some range $[\ell_1, \ell_2]$. Our heuristic is based on the assumption that the average KL-divergence increases with increasing δ and λ . This corresponds to the perturbed parameters becoming increasing dissimilar to the originals. We also assume that the user has specified some maximum value for hyperparameter δ , which we denote D . Hence $\delta \in (0, D]$.

We start by selecting initial values of δ and λ at random from their respective ranges. We evaluate the average KL-divergence for the perturbed model with these hyperparameter values. We pick one of δ or λ to change, alternating between iterations of the heuristic. If the KL-divergence is too high, we pick a value halfway between the current value of the hyperparameter and its minimum value. We evaluate using the new hyperparameters. If the KL-divergence is too low, we try again using a value a quarter of the way to the original value of the hyperparameter and its minimum value. We repeat this until we get a KL-divergence value either within the specified range or higher than the range. If it is in the range, we stop. Otherwise, we keep that value of the hyperparameter and repeat with the other hyperparameter. We perform an analogous algorithm when the KL-divergence is too high.

D EXPERIMENTAL DETAILS

D.1 QQP

We fine-tuned the `bert-base-uncased` checkpoint from the Hugging Face repository (Wolf et al., 2019) on a data set derived from the train split of QQP. This data set was simply the train split with 50k examples held out. We trained the model using Adam (Kingma & Ba, 2014) with a learning rate of 1e-5 and batch size of 32 for 40k steps.

The set of 50k examples held out from the train set were used to compute the LRM-PEFs used to learn the LRM-NPEFF decomposition. When creating the sparse approximations, we kept the 65,536 entries with the largest magnitudes for each LRM-PEF. We used the same sparsity when computing LRM-PEFs on the validation set.

We performed LRM-NPEFF on the PEFs from the held out train set examples with 256 components. We pruned entries corresponding to parameters with fewer than 8 non-zero entries across all PEFs. After initialization, we trained only G for 100 steps before performing alternating updates between W and G . The latter stage updated each factor 1500 times. We used a learning rate of 3e-5 for the G -only stage of training and a learning rate of 3e-4 for the joint stage.

D.2 NLI

We used the `connectivity/feather_berts_0` checkpoint from the Hugging Face repository as the model for our NLI experiments. This checkpoint was released as part of [McCoy et al. \(2019\)](#). It was fine-tuned on MNLI from the `bert-base-uncased` pretrained model.

We used two disjoint sets of 50k examples each from the SNLI train split to compute LRM-PEFS. When creating the sparse approximations to these PEFs, we kept the 65,536 entries with the largest magnitudes for each LRM-PEF.

We performed LRM-NPEFF on the PEFs from one of these sets using 512 components. We pruned entries corresponding to parameters with fewer than 14 non-zero entries across all PEFs. After initialization, we trained only G for 100 steps before performing alternating updates between W and G . The latter stage updated each factor 1500 times. We used a learning rate of $1e-4$ for the G -only stage of training and a learning rate of $3e-4$ for the joint stage.

D.3 VISION

We used a ResNet-50 ([He et al., 2016](#)) trained on the ImageNet classification task ([Russakovsky et al., 2015](#)), namely the `imagenet` pretrained weights of the `ResNet50` class in TensorFlow ([Abadi et al., 2016](#)).

We computed D-PEFs using 20k examples from the ImageNet train split and 30k examples from the ImageNet validation split. We only included terms with a probability of greater than $3e-3$ when performing the expectation over classes when computing the D-PEFs. When creating the sparse approximations, we kept the 65,536 entries with the largest magnitudes for each D-PEF.

We performed D-NPEFF on the PEFs from the train split using 512 components. We pruned entries corresponding to parameters with fewer than 6 non-zero entries across all PEFs. We ran NMF for 2500 steps on these D-PEFs to create the D-NPEFF decomposition.

E VISION MODEL D-NPEFF PERTURBATION DETAILS

We selected the top 128 examples for each component to compute the sign pattern. We selected the δ, λ hyperparameters such that their average KL-divergence of the top examples was between 0.25 and 0.35. The δ, λ selection process was repeated 6 times per component. For each run, we computed the ratio of the average KL-divergence for the top 128 examples of the component to the average KL-divergence across the entire set of 30k validation set examples for which we computed PEFs. We used the geometric mean of the KL-divergence ratios across these runs to get an average KL-divergence for each component.

F COMPONENTS SET EXPANSION EXPERIMENT DETAILS

Given a set of PEFs used to compute an NPEFF decomposition, we created another set of PEFs consisting of only the examples on which the model made an incorrect prediction. Expanding the set of NPEFF components on these examples is similar to computing an NPEFF decomposition, but some parameters are initialized non-randomly and some parameters are not updated during the learning process.

Divide the set of components to a group consisting of the original components and another group consisting of the new components that will be learned. The pseudo-Fishers of the former group are initialized using their values from original NPEFF decomposition and not updated during training. Their corresponding coefficients are initialized using their values from the original decomposition as well. We found that initializing these coefficients this way significantly increased the chance of the expansion learning meaningful components. The coefficients of the expanded components are initialized using the uniform distribution on $[0, 1]$. The rows of G corresponding to the expanded components are initialized using a normal distribution with zero mean and standard deviation of $\sqrt{2}/\sqrt{rm}$, where r is the sum of the number of original components and the number of components in the expansion.

Computation of the expansion proceeds in two stages with an optional third stage at the end. First, all of the coefficients are frozen while the rows of G corresponding to the new components are updated. Then perform alternate updates on the columns of W corresponding to the new components and their corresponding rows of G . The optional final stage involves performing alternating updates on all of the columns of W and updating only the rows of G corresponding to the new components.

For our experiment on the NLI model, we used a learning rate of $1e-3$ during the first stage where we were only updating the columns of G corresponding to the new components. We performed a total of 250 updates during this state. In the other stages, we used a learning rate of $3e-3$. We ran the second stage for 1000 updates of both NPEFF factors. We did not run the third stage.

G QUALITY OF SPARSE APPROXIMATION

When producing a sparse approximation to an LRM-PEF of the NLI model, we kept only 65,536 entries out of a total of about 330 million. Hence only around 0.02% of the sparse LRM-PEF’s entries are non-zero. To determine the quality of these sparse representations, we computed the Frobenius distance between a dense PEF matrix and its sparse approximation over a set of 500 examples. These distances were then normalized by dividing them by the Frobenius norm of their corresponding dense PEF matrix. We then subtract the resultant value from 1 to get a score between 0 and 1 for each example. A score of 0 indicates that the sparse approximation captures no information about the dense PEF while a score of 1 indicates a perfect match. A histogram of these scores across examples can be found at fig. 4. When keeping 65,536 entries, there is a large peak at round 0.15 in the distribution. Higher scores become less likely with only a few greater than 0.4. Increasing the number of kept entries to 262,144 shifts the peak of the score distribution to between 0.2 and 0.25. These overall results indicate that although our sparse approximations are not particular close approximations, they capture a significant amount of information given their sparsity.

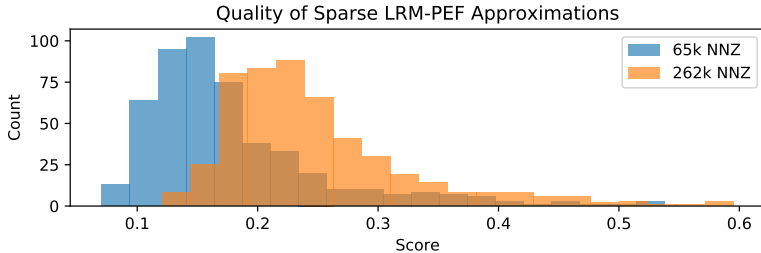


Figure 4: Histogram of per-example values indicating the closeness of the sparse approximation to SNLI LRM-PEFs. A score of 0 indicates that the approximation is identically zero while a score of 1 indicates a perfect match.

H SYNTHETIC TASK AND MODEL DETAILS

H.1 TASK DETAILS

The synthetic task can be thought of as an extremely simplified NLI task. An example looks like [BOS] Q1 S1 O1 Q2 S2 O2, which is a concatenation of a premise and hypothesis. The Q1, Q2 tokens correspond to All or Some, and a Q S O segment can be thought of as the sentence [All/Some] [subject] [verb] [object]. The verb is assumed fixed and shared between the premise and hypothesis, so it is not explicitly represented. Subjects and objects are chosen from the same set of options containing a hierarchical structure so that we can have a `is_a_subtype_of` relation between options. Each example is given a label of entails or neutral. A couple of examples in “readable” form are:

- All cows eat grass. Some bovines eat plants. \implies entails
- Some seals eat fish. All mammals eat animals. \implies neutral

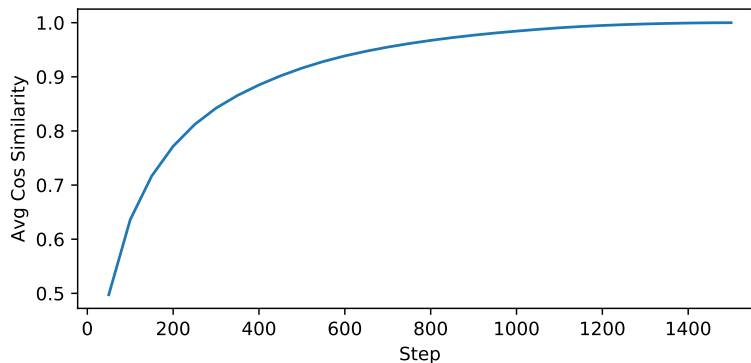


Figure 5: Average cosine similarities of component coefficients with their final values as the NPEFF decomposition progresses.

The set of options for the subjects and objects was obtained from subtree of ImageNet classes rooted at the node with id n02913152. This node corresponded to the class “building, edifice”. We did this purely to obtain a “natural-looking” hierarchy of items; the exact names of the items in their original context are not used by this task. Overall, this produced a set of 23 options.

H.2 RASP PROGRAM

RASP pseudo-code for solving the synthetic is presented in appendix H.2. The output at the last sequence position is the predicted label for the example. It solves the task with 100% accuracy.

H.3 PROGRAMMATIC DETECTION OF TUNINGS

Recall that each example will look like [BOS] Q1 S1 O1 Q2 S2 O2. For each example, we can create a set of boolean annotation depending on whether its tokens satisfy certain properties. These properties reflect the values of intermediate variables in the RASP program appendix H.2 that is implemented by the model. We then say a component is tuned to a particular property if its top 128 examples all possess that property. A breakdown of the number of components in each decomposition tuned for various properties can be found in table 1.

I TCAV

TCAV provides a means to test whether a model possesses conceptual sensitivity to a concept represented by a group of examples (Kim et al., 2018). Given activations corresponding the conceptual group and activations correspondingly to examples not from the group, TCAV learns a binary linear classifier to distinguish between the two groups. This classifier can be expressed as a vector with the same dimension as the activations that is the normal vector of the oriented hyperplane forming the decision boundary of the classifier. This is called the group’s concept activation vector (CAV). Then derivative of the log probability² for each class with respect to the activations in the direction of the CAV is computed over a set of examples. The fraction of examples with a positive directional derivative is recorded for each class to create a score. This process can be repeated multiple times using a different set of random examples to represent the examples not containing the concept. A two sided t -test can then be performed for these scores to compute a p -value for the null hypothesis of a TCAV score of 0.5.

For the TCAV experiments in this paper, we used the top 32 component/cluster examples to represent the conceptual groups. We used a random set of 128 examples to form the baseline group. We computed the TCAV for each run using a set of 5k examples. We performed 500 runs for each component/cluster.

²Note that Kim et al. (2018) uses logits while we use log probabilities.

```

1 def is_subtype_of(sop_a, sop_b):
2     token_equals_b = {t: t == sop_b for t in all_token_ids}
3     return sop_a == sop_b | reduce_or(
4         t == sop_a & reduce_or(t == token_equals_b[s] for s in supertypes
5         (t))
6         for t in item_tokens
7     )
8 def label_example(tokens):
9     # Align the hypothesis and premise.
10    hypo_aligned = tokens
11    prem_aligned = shift_by(SENTENCE_LEN, tokens)
12
13    is_prem_subtype_of_hypo = is_subtype_of(prem_aligned, hypo_aligned)
14    is_hypo_subtype_of_prem = is_subtype_of(hypo_aligned, prem_aligned)
15
16    # Use the last sequence position for a computation space.
17    is_s1_subtype_of_s2 = shift_by(1, is_prem_subtype_of_hypo)
18    is_s2_subtype_of_s1 = shift_by(1, is_hypo_subtype_of_prem)
19    is_o1_subtype_of_o2 = is_prem_subtype_of_hypo
20
21    is_all = tokens == ALL_TOKEN_ID
22    is_some = tokens == SOME_TOKEN_ID
23    is_all_q1 = shift_by(2 * SENTENCE_LEN - Q_PREM_INDEX - 1, is_all)
24    is_some_q1 = shift_by(2 * SENTENCE_LEN - Q_PREM_INDEX - 1, is_some)
25    is_all_q2 = shift_by(2 * SENTENCE_LEN - Q_HYPO_INDEX - 1, is_all)
26    is_some_q2 = shift_by(2 * SENTENCE_LEN - Q_HYPO_INDEX - 1, is_some)
27
28    # The output at the last sequence position will be the label for the
29    # example.
30    label = reduce_or(
31        ((is_all_q1 & is_all_q2) & (is_s2_subset_of_s1 &
32        is_o1_subset_of_o2)),
33        ((is_some_q1 & is_some_q2) & (is_s1_subset_of_s2 &
34        is_o1_subset_of_o2)),
35        ((is_all_q1 & is_some_q2) & (is_s2_subset_of_s1 &
36        is_o1_subset_of_o2)),
37    )
38    return label

```

Figure 6: RASP pseudo-code solving the synthetic NLI-like task.

Table 1: Number of components tuned to a particular concept from the TRACR model NPEFF runs. The concepts ending with `_item` mean that the top 128 examples for that component satisfy the corresponding relation for some fixed item. The specific item can differ from component to component. Note that many components were tuned to combinations of the more elementary concepts that we searched for.

Property	32 Comps Run	128 Comps Run
<code>o1.equals_item</code>	20	30
<code>o1.equals_o2</code>	0	8
<code>o1.strict_subtype_of_o2</code>	0	4
<code>o1_subtype_of_item</code>	2	1
<code>o1_subtype_of_o2</code>	1	0
<code>o1.supertype_of_item</code>	0	1
<code>o2.equals_item</code>	5	34
<code>o2_subtype_of_item</code>	0	2
<code>o2.supertype_of_item</code>	0	2
<code>q1.is_all</code>	0	7
<code>q1.is_all_and_q2.is_all</code>	1	3
<code>q1.is_all_and_q2.is_some</code>	1	8
<code>q1.is_some</code>	0	9
<code>q1.is_some_and_q2.is_all</code>	1	2
<code>q1.is_some_and_q2.is_some</code>	1	2
<code>q2.is_all</code>	0	8
<code>q2.is_some</code>	0	1
<code>s1.equals_s2</code>	0	1

For the LRM-PEF components and k-means clusters of the NLI model, every component had a p -value of less than $1e-23$ for at least one class. Even with a Bonferroni correction of 1500, which is the number of runs times the number of classes, every component had a statistically significant TCAV scores using any reasonable threshold.

J ADDITIONAL COMPONENT TUNINGS

J.1 NLI

Each of the sub-sections here corresponds to a single component. The top 6 examples per component are listed in descending order of component coefficient.

J.1.1 COMPONENT 0

[LABEL] **entailment** [PRED] **entailment** [COEFF] 36.0252
 [P] a brown dog is running though a river.
 [H] an animal running

[LABEL] **entailment** [PRED] **entailment** [COEFF] 33.5824
 [P] the brown dog is laying down on a blue sheet.
 [H] an animal is laying down.

[LABEL] **entailment** [PRED] **entailment** [COEFF] 33.4161
 [P] a small brown and black dog playing with a toy
 [H] an animal is playing.

[LABEL] **entailment** [PRED] **entailment** [COEFF] 32.9659
 [P] two dogs appear to be kissing with one another on flat ground.
 [H] animals are close together.

[LABEL] **entailment** [PRED] **entailment** [COEFF] 29.5676
[P] a little brown dog is running in the snow.
[H] an animal in snow.

[LABEL] **entailment** [PRED] **entailment** [COEFF] 28.6355
[P] a brown dog is standing in the water.
[H] an animal in the water

J.1.2 COMPONENT 3

[LABEL] **neutral** [PRED] **neutral** [COEFF] 21.7448
[P] a woman is taking a picture with her camera.
[H] a woman is taking a picture of a house.

[LABEL] **neutral** [PRED] **neutral** [COEFF] 21.3761
[P] a woman is pushing a red stroller down a sidewalk.
[H] a lady is pushing a stroller with three babies.

[LABEL] **neutral** [PRED] **neutral** [COEFF] 20.1738
[P] 2 women wearing brightly colored clothes are sitting next to a dirt road on a rock having a conversation while they're watching the field.
[H] 2 women sitting next to a dirt road, having a conversation about lunch last week.

[LABEL] **neutral** [PRED] **neutral** [COEFF] 19.6292
[P] a man with a large camera is taking photographs.
[H] man taking photographs of his family.

[LABEL] **neutral** [PRED] **neutral** [COEFF] 19.3897
[P] a black dog runs on the beach.
[H] a dog runs after a ball on the beach.

[LABEL] **neutral** [PRED] **neutral** [COEFF] 19.1972
[P] a man is rock climbing under a large cliff.
[H] a man is rock climbing to reach a rare plant.

J.1.3 COMPONENT 8

[LABEL] **contradiction** [PRED] **contradiction** [COEFF] 24.7734
[P] two climbers attempting to climb a steep, snow - covered peak, nearing the top, where two other climbers await them.
[H] the women are in the club singing

[LABEL] **contradiction** [PRED] **contradiction** [COEFF] 21.3290
[P] man lays prostrate on the ground on his back possibly in exhaustion.
[H] three men are playing basketball.

[LABEL] **contradiction** [PRED] **contradiction** [COEFF] 20.5294
[P] three women are standing in a field with two men in wheelchairs and hats.
[H] a group of men and women are in the office.

[LABEL] **contradiction** [PRED] **contradiction** [COEFF] 19.4801
[P] man riding a mountain bike doing a jump in the air.
[H] three women ride scooters in town.

[LABEL] **contradiction** [PRED] **contradiction** [COEFF] 17.6381
[P] group of kids wearing a blue and gray school uniform while playing.
[H] the men are racing cars.

[LABEL] **contradiction** [PRED] **contradiction** [COEFF] 16.9087
[P] a middle - eastern street vendor sells drinks to some young boys.
[H] young boys are playing soccer.

J.1.4 COMPONENT 17

[LABEL] **entailment** [PRED] **entailment** [COEFF] 7.6072
[P] gross couple kissing outdoors.
[H] a couple is kissing.

[LABEL] **entailment** [PRED] **entailment** [COEFF] 7.3462
[P] two people sitting beside a few small boats.
[H] a couple is sitting.

[LABEL] **entailment** [PRED] **entailment** [COEFF] 7.1038
[P] a bricklayer smoothing out concrete.
[H] someone is smoothing concrete.

[LABEL] **entailment** [PRED] **entailment** [COEFF] 6.6635
[P] laborers baling hay in a field.
[H] people are working with hay.

[LABEL] **entailment** [PRED] **entailment** [COEFF] 6.1639
[P] man in white facing body of water.
[H] a man is near water

[LABEL] **entailment** [PRED] **entailment** [COEFF] 5.9790
[P] a red cone on the side of a street.
[H] an object is near an edge.

J.2 VISION

Each of the sub-sections here corresponds to a single component. The top 32 examples per component are listed with component coefficient decreasing in a row-major manner from left-to-right and top-to-bottom.

J.2.1 COMPONENT 29



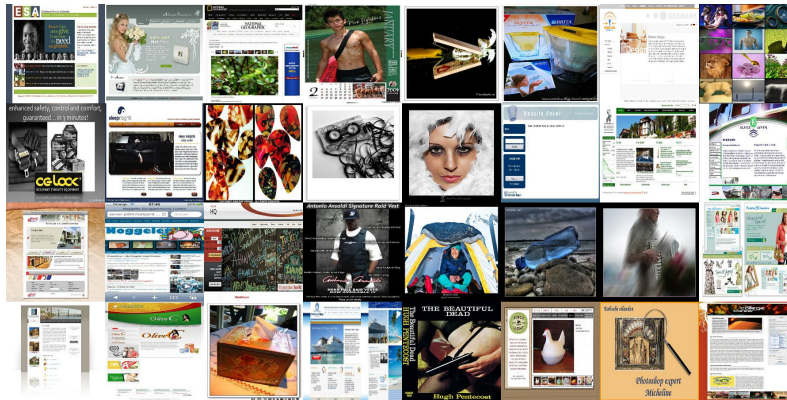
J.2.2 COMPONENT 35



J.2.3 COMPONENT 171



J.2.4 COMPONENT 276



K INCONSISTENTLY LABELED QQP COMPONENTS

K.0.1 COMPONENT 21

[LABEL] **not duplicate** [PRED] **duplicate** [COEFF] 82.3713
how do i become a travel writer?
how do you become a travel writer?

[LABEL] **not duplicate** [PRED] **duplicate** [COEFF] 70.3491
how do i become successful in my life?
how can you be successful in your life?

[LABEL] **not duplicate** [PRED] **duplicate** [COEFF] 69.6145
how do i make new friends in a new city?
how do you make friends in a new city?

[LABEL] **not duplicate** [PRED] **duplicate** [COEFF] 61.7586
how do i make my website for free?
how do you make your own website for free?

[LABEL] **duplicate** [PRED] **duplicate** [COEFF] 56.2426
how can i write a blog post on quora?
how do you write a blog on quora?

[LABEL] **duplicate** [PRED] **duplicate** [COEFF] 54.0405
how do i raise my iq?
how can you increase your iq?

[LABEL] **not duplicate** [PRED] **duplicate** [COEFF] 48.8949
what should i do to manage my time?
how do you manage your time?

[LABEL] **duplicate** [PRED] **duplicate** [COEFF] 46.0987
how do i get rid of nightmares?
how can you get rid of nightmares?

[LABEL] **not duplicate** [PRED] **duplicate** [COEFF] 45.2508
how can i get a simple mobile account number?
how do you get a simple mobile account number?

[LABEL] **duplicate** [PRED] **not duplicate** [COEFF] 43.9563
where can i find gold?
where do you find gold?

K.0.2 COMPONENT 31

[LABEL] **not duplicate** [PRED] **duplicate** [COEFF] 43.9832
what is your review of hindus?
what is your review of hinduism?

[LABEL] **not duplicate** [PRED] **duplicate** [COEFF] 39.8860
how do i convince my parents?
how can i convince my parents?

[LABEL] **not duplicate** [PRED] **duplicate** [COEFF] 32.3885
how do i get job in gulf countries?
how do i get a job in gulf country?

[LABEL] **not duplicate** [PRED] **duplicate** [COEFF] 31.6596
how is friction useful?
how is friction helpful?

[LABEL] **duplicate** [PRED] **duplicate** [COEFF] 29.7447
how do i get into iit bombay?
how to get into iit bombay?

[LABEL] **not duplicate** [PRED] **duplicate** [COEFF] 28.4342
what's the best way to read a technical book?
what is the best way to read technical books?

[LABEL] **not duplicate** [PRED] **duplicate** [COEFF] 27.7442
how do i record whatsapp call?
how do i record a whatsapp video call?

[LABEL] **duplicate** [PRED] **duplicate** [COEFF] 24.3656
how can i found local business directories in australia?
how can i find the local business directories in australia?

[LABEL] **not duplicate** [PRED] **duplicate** [COEFF] 24.0160
how do i get redeem code in google play?
how do i get a redeem code for google play?

[LABEL] **not duplicate** [PRED] **duplicate** [COEFF] 23.8029
what is the process to get a u. s. passport?
what is the process of getting a u. s. passport?

K.0.3 COMPONENT 36

[LABEL] **not duplicate** [PRED] **duplicate** [COEFF] 178.0185
how should i propose to my girlfriend?
what is the best way to propose to your girlfriend?

[LABEL] **not duplicate** [PRED] **duplicate** [COEFF] 121.0942
how do i switch my it job?
what is the best way of switching my it job?

[LABEL] **not duplicate** [PRED] **duplicate** [COEFF] 109.5911
how do i record my keyboard?
what is the best way to record a keyboard?

[LABEL] **not duplicate** [PRED] **duplicate** [COEFF] 100.9345
how should i kill myself?
what is the easiest way to kill myself?

[LABEL] **not duplicate** [PRED] **duplicate** [COEFF] 98.8751
how do you sell a car?
what is the easiest way to sell a car?

[LABEL] **not duplicate** [PRED] **duplicate** [COEFF] 81.3841
how do i kill spiders?
what is the most effective way to kill a spider?

[LABEL] **duplicate** [PRED] **duplicate** [COEFF] 75.6287
how can i kill myself?
what is the easiest way to kill myself?

[LABEL] **not duplicate** [PRED] **duplicate** [COEFF] 69.2537
how do you make money?
what is the easiest way to make money?

[LABEL] **not duplicate** [PRED] **duplicate** [COEFF] 67.5730
can i build a website on my own?
what is the best way to build your own website?

[LABEL] **duplicate** [PRED] **duplicate** [COEFF] 63.1871
how do i build muscle?
what is the best way to build muscle?

L NLI COMPONENTS WITH FAULTY HEURISTICS

L.0.1 COMPONENT 18

[LABEL] **neutral** [PRED] **entailment** [COEFF] 16.0689
[P] a young child wearing a yellow striped t - shirt and blue shorts is playing along side the lake and rocks.
[H] a young child is wearing a light yellow striped t - shirt.

[LABEL] **neutral** [PRED] **entailment** [COEFF] 15.6616
[P] young white male child with blond - hair in a red shirt coloring with crayons outside with an adult.
[H] a young white male child with blond - hair has a light red shirt.

[LABEL] **neutral** [PRED] **entailment** [COEFF] 15.4342
[P] a young woman with blond - hair, wearing a short - sleeve gray shirt and blue jean shorts, prepares food for a barbecue.
[H] a young woman has light blond - hair.

[LABEL] **neutral** [PRED] **entailment** [COEFF] 14.5433
[P] a crowd of children in green t - shirts and people holding signs and purple balloons gathers next to a building.
[H] a crowd of children has light green t - shirts.

[LABEL] **neutral** [PRED] **entailment** [COEFF] 12.1538
[P] a female baseball player wearing a blue shirt slides into base, while another player in a white shirt wearing a catcher's mitt jumps.
[H] a female baseball player is wearing a light blue shirt.

[LABEL] **neutral** [PRED] **entailment** [COEFF] 11.7806
[P] in an outdoor location with spectators in the background, a young man in a karate uniform with a blue belt has his arm around the neck of a young woman in a karate uniform with a brown belt while she grips his arm with both hands.
[H] a young man has a karate uniform with a light blue belt.

[LABEL] **neutral** [PRED] **entailment** [COEFF] 8.8071
[P] an older man in a red sweatshirt stands in front of a group of children sitting on benches in front of him.
[H] an older man in a light red sweatshirt stands.

[LABEL] **neutral** [PRED] **entailment** [COEFF] 6.1237
[P] man in yellow behind the wheel of a tractor, hooked to a trailer and under an open sided roof, while others climb on the back.
[H] a man in light yellow is behind the wheel of a tractor.

L.0.2 COMPONENT 34

[LABEL] **neutral** [PRED] **contradiction** [COEFF] 5.5193
[P] a man eating something with a spoon.
[H] a man is eating ice cream.

[LABEL] **neutral** [PRED] **contradiction** [COEFF] 3.9719
[P] a man selling many wicker chairs is pulling a cart of them through the street.
[H] a man is selling blue chairs.

[LABEL] **neutral** [PRED] **contradiction** [COEFF] 3.6611
[P] a man with a green shirt is holding a plant.
[H] a man is delivering flowers.

[LABEL] **neutral** [PRED] **contradiction** [COEFF] 3.6228
[P] a man eating a pink candy bunny.
[H] he eats a gertrude hawk easter bunny.

[LABEL] **neutral** [PRED] **contradiction** [COEFF] 3.5730
[P] two ladies selling their wares in an open market.
[H] two ladies sell their bakes goods at a farmer's market.

[LABEL] **neutral** [PRED] **contradiction** [COEFF] 3.5390
[P] an older gentleman dressed completely in white is eating from a white bowl while sitting in a large overstuffed chair.
[H] an older gentleman is eating cereal.

[LABEL] **neutral** [PRED] **contradiction** [COEFF] 3.5027
[P] a man wearing a red costume stands near others.
[H] the man is wearing a dog costume.

[LABEL] **contradiction** [PRED] **contradiction** [COEFF] 3.4998
[P] a donkey carting greens and two people on a street.
[H] a donkey is carting fruits.

L.0.3 COMPONENT 62

[LABEL] **neutral** [PRED] **entailment** [COEFF] 2.9606
[P] a person on a blue bench under a blue blanket.
[H] a person is resting.

[LABEL] **neutral** [PRED] **entailment** [COEFF] 2.8245
[P] a boy wearing khaki pants and a sports team jersey is jumping down the stairs outside.
[H] a boy is excited.

[LABEL] **neutral** [PRED] **entailment** [COEFF] 2.8070
[P] an athletic man waterskis on a lake.
[H] a fit man is having fun.

[LABEL] **entailment** [PRED] **entailment** [COEFF] 2.7448
[P] 2 girls in metal chairs are laughing together.
[H] two girls are having fun.

[LABEL] **entailment** [PRED] **entailment** [COEFF] 2.3667
[P] man in white shirt and shorts browses an item stand.
[H] a man is browsing for goods.

[LABEL] **neutral** [PRED] **entailment** [COEFF] 2.2851
[P] a gymnast in a competition is looking on with a questioning look on her face.
[H] a gymnast is confused about something.

[LABEL] **entailment** [PRED] **entailment** [COEFF] 2.2077
[P] a little girl with ponytails laughs near a plastic castle play set.
[H] a girl enjoys herself.

[LABEL] **neutral** [PRED] **entailment** [COEFF] 2.1743
[P] a woman standing in a red bikini on a outdoor sand volleyball court.
[H] a woman is playing sports.

M K-MEANS CLUSTERS TOP EXAMPLES

M.1 NLI

M.1.1 COMPONENT 1

[LABEL] **entailment** [PRED] **entailment** [COEFF] -0.0486
[P] Two chinese men looking at papers on a table.
[H] Some people are looking at papers.

[LABEL] **entailment** [PRED] **entailment** [COEFF] -0.0575
[P] Many people riding bikes on a path while another person is walking toward them.
[H] Some people are riding bikes.

[LABEL] **entailment** [PRED] **entailment** [COEFF] -0.0581
[P] A group of young people are in a garage
[H] Some people are in a garage.

[LABEL] **entailment** [PRED] **entailment** [COEFF] -0.0591
[P] A girl in a green shirt and a girl in a yellow shirt standing by water.
[H] Some girls are standing by water.

[LABEL] **entailment** [PRED] **entailment** [COEFF] -0.0614
[P] Three young people planting flowers and covering the area with a tarp.
[H] Some people are planting flowers.

[LABEL] **entailment** [PRED] **entailment** [COEFF] -0.0628
[P] A girl in a blue blouse and a girl in a green shirt sewing.
[H] Some people are sewing.

M.1.2 COMPONENT 4

[LABEL] **neutral** [PRED] **neutral** [COEFF] -0.0800
[P] A person is riding a bike in front of brick buildings.
[H] A person is riding a red bike

[LABEL] **neutral** [PRED] **neutral** [COEFF] -0.0806
[P] A firefighter dressed in gear looking puzzled.
[H] A firefighter dressed in red gear looking puzzled.

[LABEL] **neutral** [PRED] **neutral** [COEFF] -0.0824
[P] A truck - driver is working on his truck.
[H] A truck driver works on his red truck.

[LABEL] **neutral** [PRED] **neutral** [COEFF] -0.0854
[P] A young boy is sitting on a beach filling a water bottle with sand.
[H] A young boy is filling a red water bottle with sand.

[LABEL] **neutral** [PRED] **neutral** [COEFF] -0.0882
[P] Two girls sitting on a chair being sketched.
[H] Two girls sitting on a green chair are being sketched.

[LABEL] **neutral** [PRED] **neutral** [COEFF] -0.0892
[P] Three female dancers are doing dance moves on stage of an auditorium.
[H] Three female dancers, all dressed in blue, are doing dance moves in an auditorium.

M.1.3 COMPONENT 28

[LABEL] **contradiction** [PRED] **contradiction** [COEFF] -0.0535
[P] Two water polo players wrestle for the ball while a goal keeper watches in front of a goal with an angry birds advertisement on the back of the net.
[H] There is no goalkeeper in the waterpolo match.

[LABEL] **contradiction** [PRED] **contradiction** [COEFF] -0.0623
[P] Two people one person dressed in yellow and green with black boots and the other person have on white jacket and brown pants standing on the lake side with birds approaching them
[H] There are no birds at the lake.

[LABEL] **contradiction** [PRED] **contradiction** [COEFF] -0.0668
[P] People wearing glasses and shades are walking, while a man in a black shirt with the word " qualified " on it is facing them.
[H] There are no glasses

[LABEL] **contradiction** [PRED] **contradiction** [COEFF] -0.0671
[P] A family posing with a bride in a white dress at a wedding.
[H] The bride does not have a family.

[LABEL] **contradiction** [PRED] **contradiction** [COEFF] -0.0693
[P] A man plays guitar in the kitchen while a woman adjusts the dials on a dishwasher.
[H] Nobody is using the dishwasher.

[LABEL] **contradiction** [PRED] **contradiction** [COEFF] -0.0700
[P] At a party, an entertainer provides amusement to children in the form of balloon animals.
[H] There are no children at this party.

M.2 VISION

Each of the sub-sections here corresponds to a single cluster. The top 32 examples per cluster are listed with distance to cluster centroid increasing in a row-major manner from left-to-right and top-to-bottom.

M.2.1 COMPONENT 6



M.2.2 COMPONENT 19



M.2.3 COMPONENT 20

